Quantum Electronics **49** (6) 577–580 (2019)

LASER PLASMA

https://doi.org/10.1070/QEL16860

Three-channel polaro-interferometer for laser-produced plasma diagnostics with femtosecond time resolution

E.A. Bolkhovitinov, G.A. Gospodinov, K.A. Ivanov, A.A. Rupasov, A.B. Savel'ev

Abstract. **We describe an upgraded version of a three-channel polaro-interferometer, which enables laser-produced plasma probing with femtosecond time resolution. Test experiments are performed with the use of a 50-fs probe pulse and an air spark produced by a driving nanosecond laser pulse. High-contrast interference plasma images are recorded, making it possible to reconstruct the electron density plasma profile with femtosecond time resolution in a wide range of probing pulse delays relative to the driving pulse.**

Keywords: *laser-produced plasma, polaro-interferometer, interference image, time resolution.*

1. Introduction

Optical probing is among the most important and extensively used methods for investigating the dynamics of laser-produced plasma [1]. Different versions of this method provide measurements of the expansion rate and shape of opaque plasma cloud (shadowgraphing), the spatial distribution of the electron density (interferometry) and magnetic fields (polarimetry) in its transparent, subcritical region. The time resolution of all these methods is determined primarily by the duration of the probing laser pulse. The tasks associated with substance irradiation by femtosecond laser pulses at an intensity of $10^{16}-10^{22}$ W cm^{-2} [2–7] have become highly topical in recent years, the time resolution required for these studies frequently being better than 1 ps.

A three-channel polaro-interferometer was developed at the Lebedev Physical Institute (LPI) earlier. It combines all three optical probing techniques and permits determining simultaneously, in one laser pulse, the shape of the opaque plasma region, the spatial electron density profile of subcritical plasma, and the structure of spontaneous magnetic fields generated in it. The scheme developed in Ref. [8] for investigating high-temperature plasma was inherently limited at about 1 ps in probing pulse duration. This is due to the fact that the interfering beams that pass through the birefringent elements of the scheme arrive at the plane of interference pattern formation with a time delay of one of the beams relative to the other: possessing mutually orthogonal polarisations inside the birefringent analysing crystals, the beams have different phase velocities and somewhat different optical paths. This has the result that the probing pulses shorter than 1 ps cease to overlap in time in the recording plane and therefore do not interfere.

In the present work we demonstrate the possibility of improving the polaro-interferometer scheme and designing an instrument that will make it possible to probe laser-produced plasmas with femtosecond resolution and to obtain a clear interference pattern.

E.A. Bolkhovitinov, A.A. Rupasov P.N. Lebedev Physical Institute, Russian Academy of Sciences, Leninsky prosp. 53, 119991 Moscow, Russia; e-mail: bolhovitinovea@lebedev.ru;
G.A. Gospodinov Faculty of Physics, M.V. Lomonosov Moscow State University, Vorob'evy Gory, 119991 Moscow, Russia;
K.A. Ivanov, A.B. Savel'ev P.N. Lebedev Physical Institute, Russian Academy of Sciences, Leninsky prosp. 53, 119991 Moscow, Russia; Faculty of Physics, M.V. Lomonosov Moscow State University, Vorob'evy Gory, 119991 Moscow, Russia

Received 11 October 2018; revision received 31 January 2019
Kvantovaya Elektronika **49** (6) 577–580 (2019)
Translated by E.N. Ragozin

2. Polaro-interferometer scheme and its application in experiments

The polaro-interferometer was substantially improved to diagnose the high-temperature plasmas produced by laser radiation ranging widely in pulse duration (from nano- to femtoseconds) and probe the laser-produced plasmas by nano- and femtosecond laser pulses in the pulse-repetition regime (with a repetition rate of 10 Hz) on the complex of laser facilities at the International Laser Centre of the Moscow State University [7]. The instrument is based on the scheme proposed at the LPI which permits three plasma images to be obtained simultaneously: the shadow, interference, and polarisation ones (Fig. 1). These images are formed by the probing laser beam and make it possible to reconstruct the plasma electron density profile and the structure of spontaneous magnetic fields.

Three spatially separated beams are produced at the polaro-interferometer output by using birefringent wedges and polarisers: eoe (the shadow channel), oee (the polarisation channel), and eee (the beam that makes up the interference channel when it overlaps with part of the oee beam at the CCD camera). As noted above, the delay between the oee and eee beams in the CCD-array plane amounts to ~1 ps owing to the difference between the optical paths in the wedges. A natural limitation thereby arises on the probing pulse duration, which should exceed 1 ps.

When a high time resolution was not required, for a probing pulse we use a 6-ns pulse at the fundamental wavelength of a neodymium laser (1064 nm). To transit to the picosecond resolution range in plasma probing, use is made of a 2-ps long pulse at a wavelength of 400 nm, which still permitted obtaining a sufficiently high contrast of interference fringes. In order to produce such a pulse, a short femtosecond pulse was lengthened by converting it to the sec-

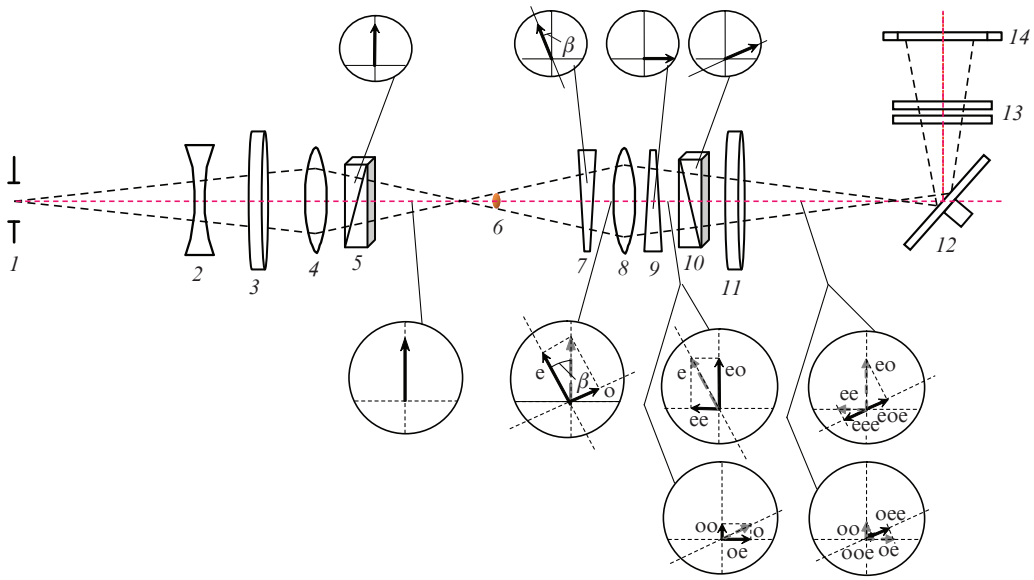

Figure 1. Optical schematic of the three-channel polaro-interferometer
(*1*) shaping diaphragm; (*2*) negative lens; (*3*, *11*) windows of the vacuum chamber; (*4*, *8*) positive lenses; (*5*, *10*) Glan prisms; (*6*) object's position and the image of the shaping diaphragm in its plane; (*7*, *9*) birefringent wedges; (12) two-mirror device which provides timing of the interfering beams; (*13*) optical filters; (*14*) CCD array camera; β is the initial decrossing angle between the optical axes of wedge *7* and Glan prism *5*. Shown in the upper part of the figure are the orientations of the optical axes of the crystals; the lower part displays vector diagrams of the beam polarisations at the corresponding points of the optical configuration. The eoe beam forms the shadow image, the beam oee forms the polarisation image, while the eee and oee beams produce the interference image.

ond harmonic in a KDP crystal of length much longer than the group length. In this case, the second harmonic pulse becomes longer, so that its duration amounted to 2 ps with the use of a 3-cm long crystal.

To study fast processes in laser-produced plasmas, a polaro-interferometer is needed, which has the highest possible time resolution, i.e. probe plasmas with a femtosecond pulse. This is hampered by the above limitation arising from the difference in optical paths between the interfering beams. To obtain a high-quality image in the interference channel when probing plasmas with femtosecond pulses, we developed a compensating device to delay one interfering beam relative to the other one using two folding mirrors (Fig. 2). The upper device mirror was fixed, while the position of the other one was adjusted with a micrometre screw. The device was placed near the focus of lens *8* (see Fig. 1), which imaged the plasma on the recording plane. This allowed the beams to be relayed to different mirrors (the eee beam was directed to the upper mirror, while the eoe and oee beams were relayed to the lower one).

The beams reflected from the mirrors were directed to the CCD camera. By adjusting the micrometre screw, it was possible to obtain in the plane of the CCD-array an interference pattern with the zone of high fringe contrast comparable to or slightly less than the overlap region of interfering images. The time resolution turned out to be comparable to the probing pulse duration and was estimated at 50 fs in the test experiments described below. In this case, the spatial resolution of the present optical system was equal to ~15 μm.

To test the new scheme, we probed the spark breakdown in the air produced by 6-ns pulses of a Nd:YAG laser, which emitted at the fundamental harmonic with a wavelength of 1064 nm and a repetition rate of 10 Hz. The output pulse energy was equal to 100 mJ. The spark breakdown was probed by the fundamental harmonic of a femtosecond

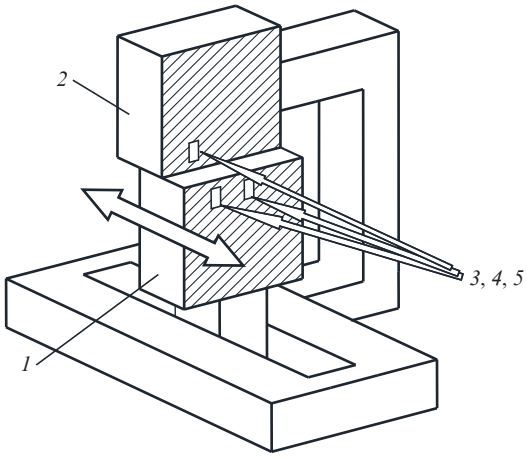

Figure 2. Optical delay device for the timing of the beams in the interference channel of the polaro-interferometer:
(*1*) mirror on a micrometre translation stage; (*2*) immobile mirror; (*3–5*) polarisation (oee) and shadow (eee, eoe) plasma images in the probing laser beam divided after passing through the birefringent wedges, which are relayed through the optical path.

Ti:sapphire laser at a wavelength of 800 nm for a pulse duration of 50 fs. The spark plasma images at the polaro-interferometer output were recorded with a CCD array camera timed to within 1 ns of the probing pulse. Figure 3 shows the images of the laser spark plasma in two polaro-interferometer channels: the polarisation and interference ones. The images were recorded for different probing pulse delays relative to the plasma-producing laser pulse, which were varied in a range of 0–40 ns.

The 15-μm width of the interference fringes makes it possible to resolve their bendings due to plasma density gradients

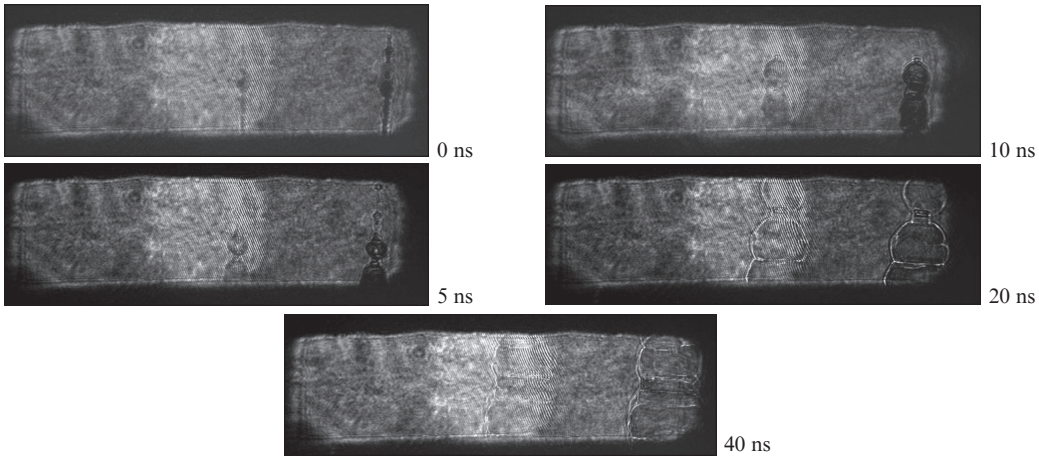

Figure 3. Images of a laser air spark in the interference (in the central part of the image) and polarisation (in the right part of the image) polaro-interferometer channels for different probing pulse delays relative to the plasma-producing laser pulse. The probing pulse duration was equal to 50 fs.

and therefore to calculate the spatial phase incursion and to reconstruct the plasma electron density profile (Fig. 4). In the context of our experiment, the critical plasma electron density N_e for the probe radiation was equal to 1.74×10^{21} cm^{-3}.

To reconstruct the electron density distribution of the laser-produced plasma, we used the algorithm based on the inverse Abelian transform. Using this approach to the processing of interference plasma images calls for the existence of axial symmetry for the electron density distribution function, which is usually realised in the interaction of laser radiation with a target in a vacuum. However, in our observations of the air laser spark, which served as a test object of the investigation, as a rule the plasma expansion was not symmetric, and so we processed part of the interference plasma image to correctly reconstruct the electron density (Fig. 4c). The resultant plasma electron density distribution of the laser air spark

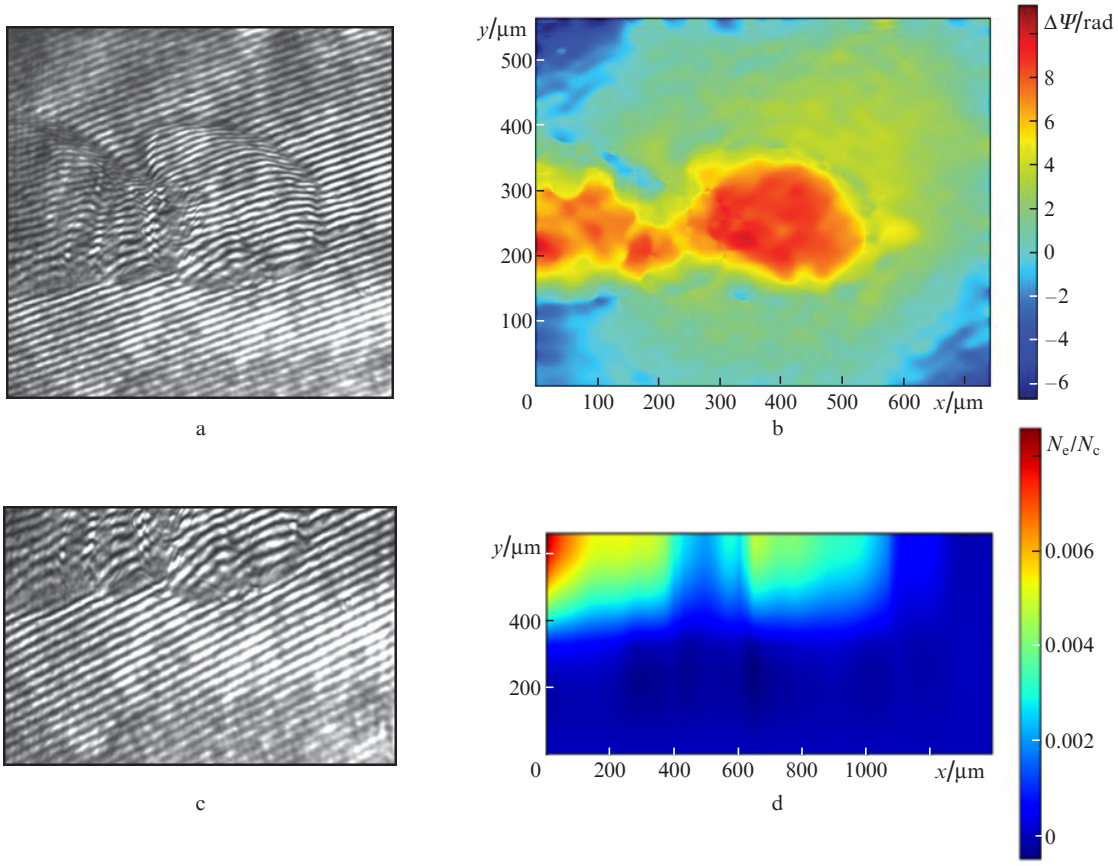

Figure 4. (a) Interference pattern of laser air spark plasma, (b) reconstructed phase shift distribution $\Delta\Psi$, (c) processed part of the interference discharge image, and (d) profile of the electron plasma density in fractions of N_c computer-reconstructed for this image part. The probing pulse duration is equal to 50 fs and its delay relative to the plasma-producing laser pulse is equal to 20 ns.

is shown in Fig. 4d for a 20 ns delay of the probing pulse relative to the plasma-producing pulse.

Therefore, we have improved the three-channel polaro-interferometer using a delay line for one of the interfering beams. The delay line uses two mirrors and a micrometre translation stage. The updated scheme was shown to form clear interferometer images, which makes it possible to reconstruct the profile of the plasma electron density with a time resolution of up to 50 fs.

Acknowledgements. This work was supported in part by the Russian Foundation for Basic Research (Grant No. 16-02-00302-a).

References

1. Basov N.G., Zakharenkov Yu.A., Rupasov A.A., Sklizkov G.V., Shikanov A.S. *Diagnostika Plotnoi Plazmy* (Dense Plasma Diagnostics) (Moscow: Fizmatlit, 1989) Ch. 2.
2. Gibbon P. *Short Pulse Laser Interactions with Matter* (London: Imperial College Press, 2005).
3. Mourou G., Tajima T., Bulanov S. *Rev. Modern Phys*., **78**, 309 (2006).
4. Andreev A.V., Gordienko V.M., Savel'ev A.B. *Kvantovaya Elektron*., **31**, 941 (2001) [*Quantum Electron*., **31**, 941 (2001)].
5. Uryupina D.S., Ivanov K.A., Brantov A.V., Savel'ev A.B., Bychenkov V.Yu., Povarnitsyn M.E., Volkov R.V., Tikhonchuk V.T. *Phys. Plasmas*, **19**, 013104 (2012).
6. Nakatsutsumi M., Sentoku Y., Korzhimanov A., Chen S.N., Buffechoux S., Kon A., Atherton B., Audebert P., Geissel M., Hurd L., Kimmel M., Rambo P., Schollmeier M., Schwarz J., Starodubtsev M., Gremillet L., Kodama R., Fuchs J. *Nat. Commun*., **280** (9), 1 (2018).
7. Krestovskikh D.A., Ivanov K.A., Tsymbalov I.N., Shulyapov S.A., Bukin V.V., Volkov R.V., Rupasov A.A., Savel'ev A.B. *Kvantovaya Elektron*., **47**, 45 (2017) [*Quantum Electron*., **47**, 45 (2017)].
8. Bolkhovitinov E.A., Krayushkin I.A., Rupasov A.A., Fedotov S.I., Shikanov A.S. *Prib. Tekhn. Eksp*., (3), 101 (2007).